A Micromechanical Damage Model of Ceramic for Shock Loading

Huilan Ren ,Jianguo Ning
State Key Laboratory of Explosion Science and Technology, Beijing Institute of Technology, Beijing 100081, China,e-mail:huilanren@bit.edu.cn

ABSTRACT. *A damage model applicable to ceramics subjected to dynamic compressive loading has been developed. The model was based on damage micromechanics and wing crack nucleation and growth. Tension wing cracks nucleated and propagated from the tip of the sliding cracks in the direction of maximum applied compression when the stress-intensity factor reached its critical value. The rate of crack growth was governed by a universal relation in dynamic fracture for high strain rate. The failure of the material was linked to a critical density of damage. The model predicted the failure or peak strength to increase with increasing shock loading. The results of the dynamic damage evolution model were compared with the experimental results and a good agreement was found.*

INTRODUCTION

Ceramic materials carry many initial defects, such as grain boundaries, micro-cracks, and pores. Under compressive loads, secondary cracks are induced around these defects. Through scanning electron microscope and acoustic emission examinations, the growth and nucleation of these cracks are revealed to dominate the failure and macroscopic mechanical properties of the ceramic materials [1,2]. After these observations, researchers began to focus more on the behaviors of cracks through experimental and analytical methods in an effort to study the mechanical properties of ceramic materials under compressive loads. Several micromechanics-based cracks models have been proposed since[3-6]. G.Ravichandran[7] presented the micromechanical model for aluminum nitride in the strain rate range of $5\times10^{-6}\sim2\times10^{3}s^{-1}$. The model was based on non-interacting sliding micro-cracks that were uniformly distributed in the material and predicted the failure or peak strength to increase with increasing strain rate. Deng and Nemat-Nasser[8] studied the constitutive behavior of brittle materials subjected to compressive loading has been under stress pulse loading.

The objective of paper is to develop a micromechanical damage model based on the nucleation and growth of wing cracks for alumina under high strain rate.

CONSTITUTIVE MODEL

Sliding crack model

The sliding crack model as a mechanism has been widely accepted to study brittle materials under compressive loads. As shown in Fig. 1, an initial crack, at a length of $2c$, oriented at angle γ with respect to the σ_1 direction, and a pair of curved tensile cracks, nucleate at the tips of the preexisting model flaw and grow with the increase of compression and finally become parallel to the direction of the maximum far-field compression.

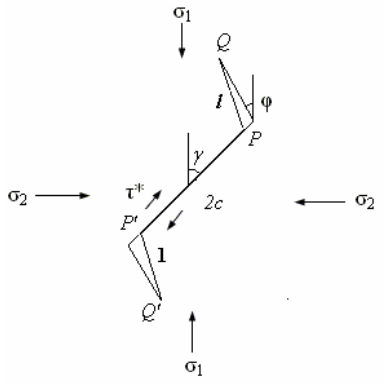

Figure 1. Sliding crack model

When the local resolved shear stress along the crack plane exceeds the threshold shear friction, sliding occurs. With a continued increase in applied compressive load, the growth of a tensile crack will be initiated when the stress intensity factor K_I of the tensile crack equal to the model Ⅰ fracture toughness. Assuming no interaction existing between cracks, the stress intensity factor at the tip of sliding crack can be written as

$$K_I = \frac{F \sin\theta}{\sqrt{\pi(l + l^*)}} - \sigma_2 \sqrt{\pi l} \tag{1}$$

where F represents the effective sliding force on the crack plane, $F = 2c\tau^*$, and l is the tensional crack length, $l^* = 0.27c$.

Crack nucleation and growth criterion

Assume that the micro-cracks growth is governed by a critical stress intensity factor, and the growth will be sustained provided that

$$K_{ID} = K_{IC}^D \tag{2}$$

where K_{ID} is the dynamic stress intensity factor, and K_{IC}^{D} is the dynamic fracture toughness, which is assumed to be independent to the strain rate.

The stress intensity factor that drives the growth of wing cracks of the length K_{ID} is a function of the current length of crack l and the velocity of cracks growth $\dot{l}$. So we can write

$$K_{ID}(l,\dot{l}) = k(\dot{l})K_I(l,0) \tag{3}$$

where

$$k(\dot{l}) = \left(1-\frac{\dot{l}}{C_R}\right)\left(1-\frac{\dot{l}}{2C_R}\right)^{-1} \tag{4}$$

The cracks grow by either the increasing compression or the nucleation of cracks. The nucleation of cracks is assumed to satisfy the Weibull distribution [9]

$$N = k\varepsilon^m \tag{5}$$

where N is the number of micro-cracks; k, m are the material parameters.

Many experimental results indicated that the nucleation, growth, and interaction of micro-cracks played an important role in the damage and failure of brittle materials. Under axial strain compression, the fracture mechanism is very complicated corresponding to the confining pressure. It has been revealed that brittle materials fail via axial splitting under axial compression when the confining pressure is zero or close to zero, or via the shear failure when the confining pressure is moderate and still below the brittle-ductile transition value [3].

A body cell containing a sliding crack is considered under applied biaxial compression. The induced axial and lateral strains are ε_1 and ε_2, respectively. The induced strains can be divided into two parts as:

$$\begin{Bmatrix}\varepsilon_1\\ \varepsilon_2\end{Bmatrix} = \begin{Bmatrix}\varepsilon_1^e+\varepsilon_1^d\\ \varepsilon_2^e+\varepsilon_2^d\end{Bmatrix} \tag{6}$$

where ε_1^e and ε_2^e are elastic strains associated with the alumina material without cracks under compressive stress, and ε_1^d and ε_2^d are non-elastic due to the growth of the sliding cracks.

The elastic strains can be written as

$$\begin{Bmatrix}\varepsilon_1^e\\ \varepsilon_2^e\end{Bmatrix} = \frac{(k+1)(v+1)}{4E}\begin{pmatrix}1 & \frac{k-3}{k+1}\\ \frac{k-3}{k+1} & 1\end{pmatrix}\begin{pmatrix}\sigma_1\\ \sigma_2\end{pmatrix} \tag{7}$$

where E and v are the Young's modulus and Poisson's ratio of alumina, respectively, at $k = 3-4v$ for the plane strain condition.

The non-elastic strains are derived by the energy equilibrium equation shown below. According to the body containing a sliding crack shown in Fig. 1 under compressive loads, the energy equilibrium equation is

$$W_1 = 2U_e + W_f \tag{8}$$

where W_1 is the work / energy performed by the applied loads, U_e is the energy dissipated by the growth of tensile cracks, and W_f is the frictional dissipation energy due to the sliding of the initial crack.

Under fixed loading conditions, the work done by the applied loads σ_1, σ_2 on the additional displacements is

$$W_1 = 4bh(\sigma_1 \Delta\varepsilon_1 + \sigma_2 \Delta\varepsilon_2) \tag{9}$$

where $4bh$ is the volume of a unit thickness cell, and $\Delta\varepsilon_1, \Delta\varepsilon_2$ are the strain increments in ε_1 and ε_2 due to each crack, respectively.

Based on the linearity of the problem under consideration, the strains increments ($\Delta\varepsilon_1$ and $\Delta\varepsilon_2$) due to the growth of the sliding crack are assumed to be linearly dependent on the applied compressive stress σ_1 and σ_2 as

$$\begin{pmatrix} \Delta\varepsilon_1 \\ \Delta\varepsilon_2 \end{pmatrix} = \begin{bmatrix} S_{11} & S_{12} \\ S_{21} & S_{22} \end{bmatrix} \begin{pmatrix} \sigma_1 \\ \sigma_2 \end{pmatrix} \tag{10}$$

where $S_{ij}(i, j = 1, 2)$ are constants and $S_{12} = S_{21}$.

The work done by the applied loads is then

$$W_1 = 4bh(S_{11}\sigma_1^2 + 2\sigma_1\sigma_2 S_{12} + S_{22}\sigma_2^2) \tag{11}$$

There are two crack tips in the model. The strain energy dissipated at each crack tip can be expressed by a stress intensity factor K_I

$$U_e = 2U_c = 2\int_0^l \frac{(k+1)(v+1)}{4E} K_I^2 dl \tag{12}$$

Substituting Eq. (1) into Eq. (12) and then integrating it, the strain energy can be given as

$$\begin{aligned} U_e = \frac{(k+1)(1+v)}{2E} \Bigg\{ & \frac{4c^2(\tau^*)^2 \sin^2\theta}{\pi} \ln\left(\frac{l+l_*}{l_*}\right) + \frac{1}{2}\sigma_2^2 \pi l^2 \\ & -2c\tau^*\sigma_2 \sin\theta \left(\ln\left(\sqrt{\frac{l}{l_*}} + \sqrt{1+\frac{l}{l_*}}\right) - \sqrt{\frac{l}{l_*}\left(1+\frac{l}{l_*}\right)} \right) \Bigg\} \end{aligned} \tag{13}$$

Under the shear stress ignoring the crack spacing the sliding displacement δ can be written as [7]

$$\delta = \frac{(k+1)(1+v)}{2E\sin\theta} \left(\frac{2c\tau^* \sin\theta}{\sqrt{\pi(l+l_*)}} - \sigma_2\sqrt{\pi l} + \sigma_2\sqrt{\frac{\pi l}{2}} \right) \sqrt{2\pi(l+l_{**})} \tag{14}$$

Then frictional dissipation energy due to sliding of the initial crack is then

$$W_f = 2c\tau_f\delta = \sqrt{2}c\frac{(1+k)(1+v)}{E}\left\{\sigma_1^2\left(\frac{1}{2}\mu c\sin 2\theta - \frac{1}{4}\mu c\sin 4\theta - 2\mu^2\sin^4\theta\right) + \right.$$
$$\sigma_2^2\left(\frac{1}{4}\mu c\sin 4\theta - \frac{1}{2}\mu c\sin 2\theta - 2\mu^2 c\cos^4\theta + \frac{1-\sqrt{2}}{2\sqrt{2}}\mu\pi\cos\theta\sqrt{l(l+l_{**})}\right) \quad (15)$$
$$\left. + \sigma_1\sigma_2\left(\frac{1}{2}\mu c\sin 4\theta - \mu^2 c\sin^2\theta + \frac{1-\sqrt{2}}{2\sqrt{2}}\mu\pi\sin\theta\tan g\theta\sqrt{l(l+l_{**})}\right)\right\}$$

Based on Eqs. (8), (11), (13), and (15), S_{11}, S_{12}, S_{22} can be solved by comparing the coefficients of the quadratic terms as

$$S_{11} = \frac{(1+k)(1+v)}{E}\frac{1}{4bh}(A_1B_1 + C_1) \quad (16a)$$

$$S_{22} = \frac{(1+k)(1+v)}{E}\frac{1}{4bh}(A_1B_2 + C_2 + A_2D_1 + A_3 + A_4C_3) \quad (16b)$$

$$S_{12} = \frac{(1+k)(1+v)}{E}\frac{1}{4bh}(A_1B_3 + B_4 - A_4C_4 + A_5C_5) \quad (16c)$$

The coefficients of A_1, A_2, A_3, A_4, A_5 related to the length of tensional crack l, $B_1, B_2, B_3, B_4, C_1, C_2, C_3, C_4, C_5, D_1$ related to the initial crack length $2c$, and crack orientation θ were given in the reference[10].

For a body containing N sliding cracks, and if crack interactions are not considered, the total non-elastic strain can be calculated as $N\times\begin{pmatrix}\Delta\varepsilon_1\\ \Delta\varepsilon_2\end{pmatrix}$, the total strains induced from the applied compressive loads can be calculated by

$$\begin{pmatrix}\varepsilon_1\\ \varepsilon_2\end{pmatrix} = \begin{pmatrix}\varepsilon_1^e + \varepsilon_1^d\\ \varepsilon_2^e + \varepsilon_2^d\end{pmatrix} = \frac{(k+1)(1+v)}{4E}\begin{pmatrix}1 & \frac{k-3}{k+1}\\ \frac{k-3}{k+1} & 1\end{pmatrix}\begin{pmatrix}\sigma_1\\ \sigma_2\end{pmatrix} + N\begin{pmatrix}S_{11} & S_{12}\\ S_{12} & S_{22}\end{pmatrix}\begin{pmatrix}\sigma_1\\ \sigma_2\end{pmatrix} \quad (17)$$

Under dynamic uniaxial compressive loads, $\varepsilon_2 = 0$, and the constitutive relationship of the alumina is reduced to the following forms

$$\varepsilon_1 = \frac{(k+1)(1+v)}{4E}\left(\sigma_1 + \frac{k-3}{k+1}\sigma_2\right) + N\left(S_{11}\sigma_1 + S_{12}\sigma_2\right) \quad (18)$$

Under uniaxial strain conditions, lateral stress $\sigma_2 = (1-v)/(1-2v)\sigma_1$, and then the constitutive relationship with respect to the σ_1 direction can be given as

$$\varepsilon_1 = \frac{(1+v)(1-2v)}{(1-v)E}\left(\sigma_1 + N\times(A_1B_1 + A_1B_3 - A_4C_4 + A_5C_5 + C_1 + B_4)\sigma_1\right) \quad (19)$$

Analysis and results

Figure 2 shows that the failure stress and failure strain decrease with the increase of k. An increase in the value of m causes a decrease in the number of active micro-cracks per unit volume, and the fracture strength should increase with increasing m. From Fig.2, both the failure stress and failure strain decrease with the increase of the initial crack size, which has strong influences over the failure strength. The larger initial pre-flaws of the material, the easier to produce micro-cracks and to decrease the failure strength.

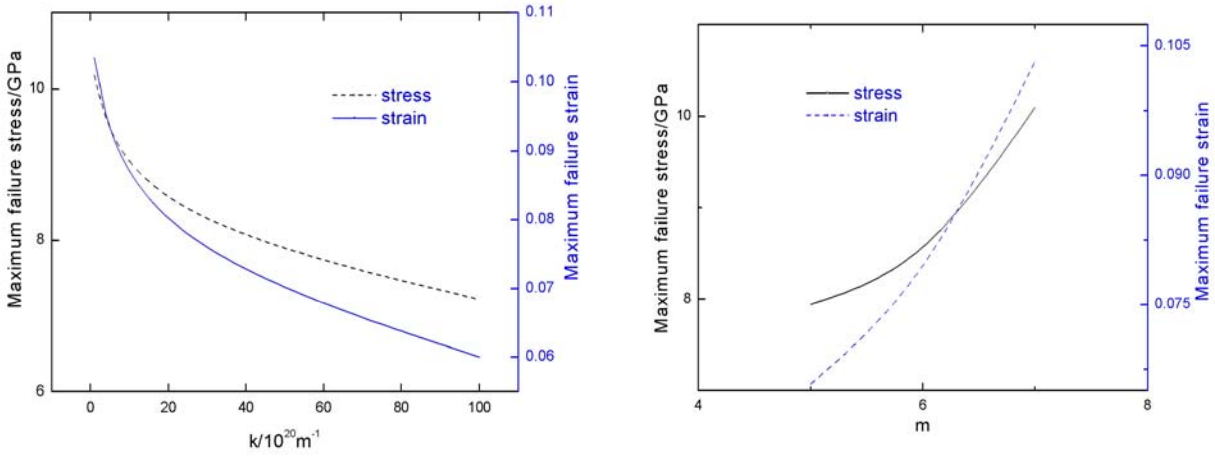

Figure 2 Influence of parameters k and m on failure stress and failure strain

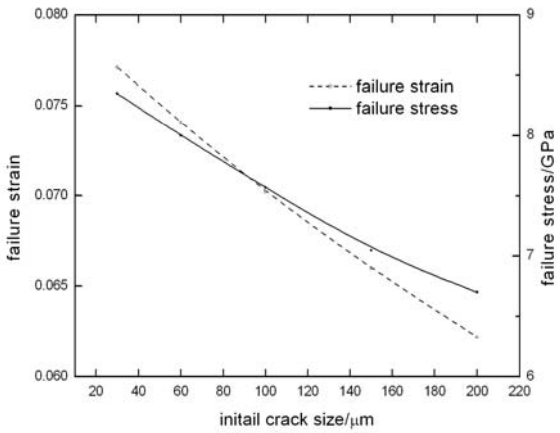

Figure 3 The influence of initial crack length on failure stress and failure strain

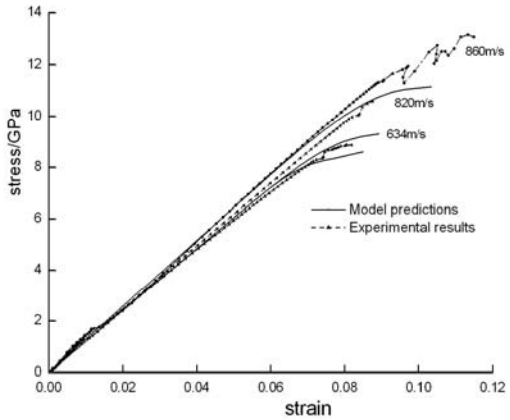

Figure 4 Comparison of experimental results and model prediction

To validate the model predications, the stress-strain curves of uniaxial strain

compression under dynamic loading are calculated based on the constitutive model. The results of the Lagrange analysis are used as the experimental stress-strain curves under unixial strain compressions[11-12]. The strain rate is about $10^5 s^{-1}$. Several parameter values, such as $k, m, 2c, \mu$, are chosen appropriately. The initial crack length is set the same as the grain size. In calculations here, $k = 10^{19}, m = 6, 2c = 60\mu m, \mu = 0.7$ are adopted. The dynamic failure toughness K_{ID} is assumed to be static K_{IC}. The Young's modulus and Poisson's ratio of the alumina are set as 120 GPa and 0.228, respectively, in the present analysis. Fig. 4 shows the stress-strain curves of the alumina at a high strain rate from the micromechanical modeling and it reveals that the stress-strain curve is likely to be elastic during the initial stage and then seems to be non-elastic due to the crack nucleation and the growth of the cracks under higher pressure. The constitutive model predictions appear to agree well with the experimental results.

CONCLUSIONS

The micromechanical constitutive model was developed to study the mechanical properties of the alumina under dynamic multi-axial compressive loading. The model took into account of the nucleation and growth of cracks. The crack growth law was derived based on dynamic fracture mechanisms. The effects of parameters of both the micro-cracks nucleation and the initial crack size on the dynamic fracture strength were discussed. The stress-strain curves obtained from the micromechanical model agree well with the experimental results.

REFERENCES

1.F.Longy, J.Cagnoux . 1989.*J. Am. Ceram*72(6),971-979
2. H.D.Espinosa,G.Raiser,R.J.Clifton.1992.*Journal of Hard Materials*3(3-4),285-313
3.S.Nemat-Nasser,H.Deng. 1994 .*Acta. Metal.Mater*42(3),1013-1024
4. C.Y. Huang,C.Subhash,S.J.Vitton. 2002. *Mech. mater*34,267-277S.
5. H.B Li, J .Zhao, T.J.Li . 2000.*Inter. J. Rock Mechan. Mining Sci*37, 923-935.
6. H. Horri, S. Nemat-Nasser 1986. *Phil. Trans. Royal Soc*319, 337-374.
7.G.Ravichandran and G.subhash. 1995.*Int. J. Sol. S*32(17/18),2627-2646
8. S.Nemat-Nasser,H.Deng. 1987. *J. Geo. Res*.6805-6821
9. A.M. Rajendran, J.L. 1989.*J. Appl. Phys*66(8), 3560-3565.
10.H.L.Ren. (2006). Thesis,Beijing Institute of Technology ,China
11.J.G.Ning,H.L.Ren,P.Li. 2008.*Acta Mech Sin*24:305-315
12. H.L.Ren,P.Li.2006. *Key engineering materials* Vols 340-341:289-294